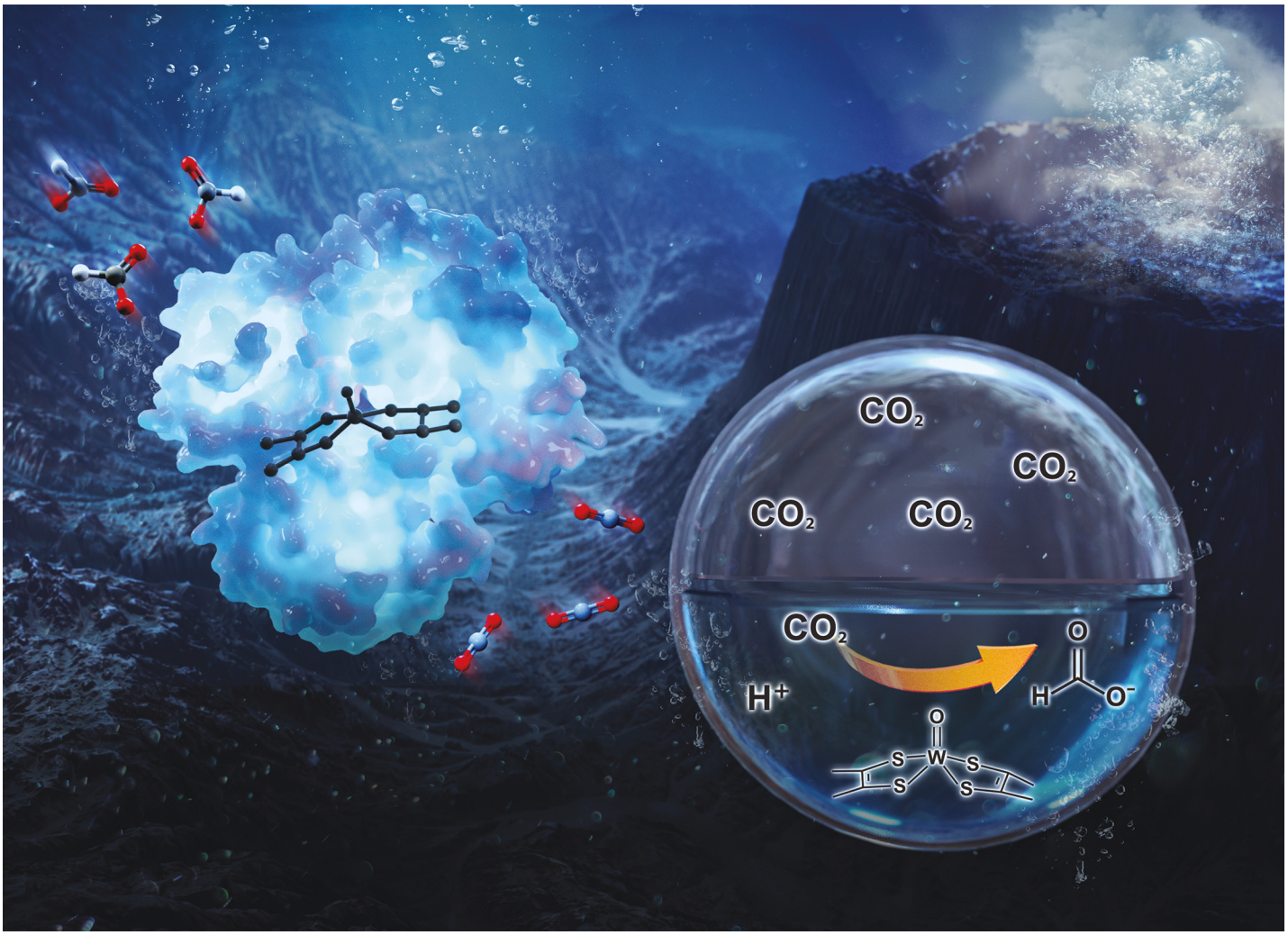

Showcasing research from Professor Junhyeok Seo's laboratory, Department of Chemistry, Gwangju Institute of Science and Technology, Gwangju, South Korea.

Reactivity of a biomimetic W(IV) bis-dithiolene complex with CO_2 leading to formate production and structural rearrangement

A mononuclear W(IV) bis-dithiolene complex, analogous to the W-dependent formate dehydrogenase active site, reduces CO_2 to formate while generating a dinuclear W(V) complex. During the reaction, an unusual structural rearrangement provides a novel triply bridged dinuclear tungsten complex.

As featured in:

See Junhyeok Seo, Eunsuk Kim *et al.*, *Dalton Trans.*, 2019, **48**, 17441.

ROYAL SOCIETY OF CHEMISTRY | Celebrating IYPT 2019

rsc.li/dalton

Registered charity number: 207890

Dalton Transactions

COMMUNICATION

View Article Online
View Journal | View Issue

Cite this: *Dalton Trans.*, 2019, **48**, 17441

Received 3rd October 2019,
Accepted 10th November 2019

DOI: 10.1039/c9dt03906f

rsc.li/dalton

Reactivity of a biomimetic W(IV) bis-dithiolene complex with CO_2 leading to formate production and structural rearrangement†

Junhyeok Seo, *[a] Jason Shearer,[b] Paul G. Williard[c] and Eunsuk Kim *[c]

A mononuclear W(IV) bis-dithiolene complex stabilized by an oxo ligand shows a reductive reactivity toward CO_2, from which formate and a dinuclear W(V) complex are generated. An unusual structural rearrangement was observed during the reaction. Structural and spectroscopic characterization for a novel triply bridged dinuclear W(V) complex is reported.

In the current energy system using fossil fuels, the utilization of CO_2 attracts substantial research interest because the conversion of combustion waste to valuable industrial products can reduce the emission of unwanted gases into the air.[1–4] The science and technology for CO_2 capture and conversion are continually developing, although the poor reactivity of CO_2 makes the chemical transformation quite challenging. Considerable efforts have been made to develop transition-metal based catalysts and electrocatalysts for CO_2 conversion,[3,5] among which tungsten complexes have shown versatile reactivity.[6–12] Selected examples include a low-valent tungsten complex to form a W–CO_2 adduct such as μ_2-η^3 type W–CO_2–Li in the presence of Lewis acid,[13] a zero-valent tungsten phenoxide complex to form phenyl carbonate *via* a reversible insertion of CO_2,[14] and a tungsten carbonyl complex to generate a tungsten hydrido-carbonate or hydrido-carbamate from CO_2 with excess methanol or secondary amine.[15] In addition, a tungsten-hydride $HW(CO)_5^-$ is known to react with CO_2 to produce formate.[16]

In nature, there exist tungsten containing formate dehydrogenases (W-FDHs) which reversibly convert formate to CO_2 (formate ⇄ CO_2 + H^+ + $2e^-$) (Fig. 1).[17] Unlike the aforementioned synthetic CO_2 activating complexes, the tungsten ion in the W-FDH remains in high valencies, alternating between +4 and +6 oxidation states during the catalytic cycle. Hirst *et al.* reported that purified Mo/W-FDH proteins exhibited superb electrocatalytic activity, in which the conversion of CO_2 to/from formate was achieved around a thermodynamic potential of −0.49 V *vs.* NHE.[18,19]

The W centre in the FDH is stabilized by two redox non-innocent pyranopterin dithiolate ligands (Fig. 1).[17] A group of bis(dithiolene)tungsten FDH model complexes that closely imitate the enzyme active site structure have been synthesized.[20] There is also a reported model complex for the formate-bound form, $[WO(HCO_2)(S_2C_2Me_2)_2]^-$.[21] The most studied chemical reactivity of the FDH model complexes is oxygen atom transfer (OAT) chemistry.[22] Holm *et al.* reported that $[W^{IV}O(S_2C_2Me_2)_2](Et_4N)_2$ (**1**) undergoes OAT with trimethylamine N-oxide (Me_3NO) to yield Me_3N and the corresponding dioxo species, $[W^{VI}(O)_2(S_2C_2Me_2)_2](Et_4N)_2$.[23] Majumdar *et al.* reported a similar OAT of $[W^{IV}O(S_2C_2(CN)_2)_2]^{2-}$ using Me_3NO.[24] Sarkar *et al.* showed that $[W^{IV}O(S_2C_2(CN)_2)_2]^{2-}$ reacts with HCO_3^- to give $[W^{VI}(O)_2(S_2C_2(CN)_2)_2]^{2-}$ and HCO_2^- in aqueous media.[25] In addition to the OAT, complex **1** can be oxidized by iodine to form a one-electron oxidized analogue, $[W^{V}O(S_2C_2Me_2)_2]^-$.[23] However, an enzyme-like CO_2/formate conversion has not been reported with these FDH model complexes to date.

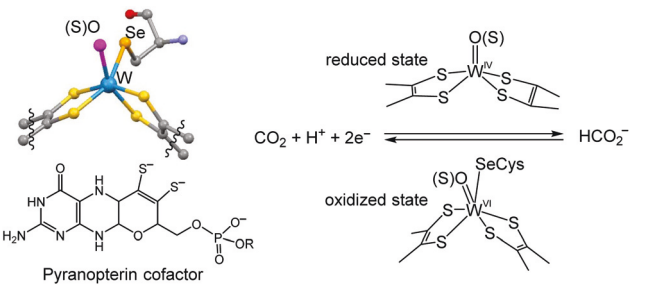

Fig. 1 (left) The active site structure of the W-FDH in the oxidized state (*Desulfovibrio gigas*, PDB ID: 1H0H); (right) the reversible conversion of CO_2 to formate catalysed by the active site.

[a]*Department of Chemistry, Gwangju Institute of Science and Technology, Gwangju 61005, Republic of Korea. E-mail: seojh@gist.ac.kr*
[b]*Department of Chemistry, Trinity University, San Antonio, Texas 78121, USA*
[c]*Department of Chemistry, Brown University, Providence, Rhode Island 02912, USA*

†Electronic supplementary information (ESI) available. CCDC 915866. For ESI and crystallographic data in CIF or other electronic format see DOI: 10.1039/C9DT03906F

We have investigated the reactions between W(IV) bis-dithiolene complexes and gaseous CO_2. In the previous isotopic labelling experiments,[26] we observed that a biomimetic bis-dithiolene W^{IV}–OH species reacted with CO_2 to form a W-(bi)carbonate intermediate indicating a direct interaction between the high-valent W^{IV} centre and the oxygen of gaseous CO_2.[26] This was encouraging because a computational study suggested that a M-thiocarbonate intermediate could form prior to the generation of the M-formate (M = Mo or W) during the catalytic cycle of FDHs,[27] although another pathway of leaving a thiocarbonate moiety attached to the cysteine residue has been proposed elsewhere.[28] However, our previous model system did not proceed with the following reduction step to form formate or other reduced CO_2 species.[26] Here, we report the CO_2 reactivity of the bis(dithiolene) W^{IV}=O complex, which leads to the generation of formate at elevated temperatures (*e.g.*, 90 °C). Our efforts to investigate the thermal reactivity of this complex were inspired by natural conditions, in which the W-FDHs thrive at hydrothermal vents. Although there has been a report on the correlation between temperature and the electrochemical behaviours of Mo- or W-dithiolene complexes,[29] the temperature-dependent chemical reactivity of the FDH model complexes has not been reported to date.

A W^{IV} bis-dithiolene complex stabilized by an oxo ligand, $[W^{IV}O(S_2C_2Me_2)_2]^{2-}$ (**1**), is quite robust even at elevated temperatures in solution. No sign of decomposition was observed when **1** was heated in acetonitrile at 90 °C under Ar over several days. When the acetonitrile solution of **1** was exposed to gaseous CO_2 (2 atm) at room temperature, **1** did not show any reactivity even after several days. However, changing the reaction temperature to 90 °C completely converted **1** to a new, unexpected dinuclear complex, $[W^{V}_2O_2(\mu\text{-}S)(\mu\text{-}S_2C_2Me_2)(S_2C_2Me_2)_2](Et_4N)_2$ (**2**) over 4 days (Scheme 1). Product **2** was isolated in 86% yield as an orange solid. The **1**-to-**2** conversion was accompanied by an asymmetric bond cleavage of the W–S and C–S bonds in one of the dithiolene ligands, leaving a dimethylthiirene fragment as another reaction product, which was detected by GC-MS (Fig. S1†). This type of dithiolene ligand cleavage has never been reported previously. Along with the oxidative conversion of **1** to **2**, remarkably, gaseous CO_2 reduced by two electrons formed formate (HCO_2^-) (*vide infra*).

X-ray analysis of the single crystal of **2** reveals triply bridged dinuclear tungsten centres by a μ-sulfide and a μ-dithiolene ligand (Fig. 2). Each W centre is in a distorted octahedral geometry. A W–W distance of 2.823(8) Å and a small W1–S–W2 angle of 68.18° suggest a direct metal–metal interaction. DFT calculations confirm that the W–W bond is in the ground state, where the d_{xy} orbitals of the two tungstens at the HOMO level overlap very well due to the high degree of symmetry (Fig. S2†). The W–W bond distance is considerably shorter by ~0.2 Å than the doubly bridged W···W (3.000 Å) distance of the $[W^{V}_2(\mu_2\text{-}S)_2(S_2C_2Me_2)_4]^{2-}$ complex.[23] Each W^{V}=O bond distance (~1.72 Å) of **2** lies in a typical range of W^{V}=O bond distance.[30] The quasi-symmetric W^{V}=O bond of **2** in the *syn* conformation shows a strong infrared stretch frequency of 918 cm^{-1}, which is 23 cm^{-1} higher than that of the W^{IV}=O (895 cm^{-1}) of **1** (Fig. S3†). The peripheral dithiolate ligand coordinates to the W ion asymmetrically. The W1–S5 bond *trans* to μ-S7 is measured to be 0.024 Å longer than that of the W1–S6 bond, and a similar trend is observed in the W2 centre (W2–S1 2.399(2); W2–S2 2.422(3) Å). A strong *trans* influence is observed in the μ-dithiolate ligand, where the W–S4 bond *trans* to W=O is elongated severely by 0.24 Å in comparison with W–S3. The bridging and peripheral dithiolate ligands were also distinguished in the solution NMR spectrum. The ^{13}C NMR (CD_3CN) spectrum of **2** shows two sets of dithiolates (Fig. S4†).

Redox non-innocent dithiolene is interconvertible among three possible oxidation levels, ene-1,2-dithiolate $(S_2C_2R_2)^{2-}$ ↔ thienyl radical anion $(S_2C_2R_2)^{-\bullet}$ ↔ 1,2-dithione.[31,32] The dithiolene ligand of **2** can be identified by measuring the dithiolene backbone distances.[33] The C–C (1.32–1.35 Å) and C–S (1.75–1.80 Å) bond distances of the bridging and peripheral dithiolene of **2** suggest the fully reduced dithiolates.[33] Accordingly, the oxidation states of both the W ions are assigned as the W^{V} state. The S K-edge X-ray absorption spectrum and the complementary simulation data suggest the relatively low covalency of the W d-orbital with the p orbital of S from dithiolene, and moderate S-character is observed in the bridging sulfide (Fig. S5†). It is due to the relative hardness of the W^{V} ion.

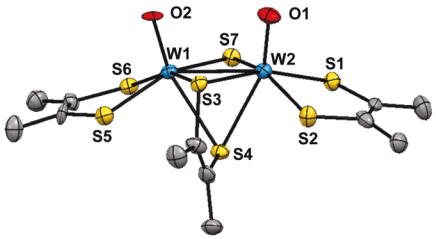

Fig. 2 The molecular structure of $[W_2O_2(\mu\text{-}S)(\mu\text{-}S_2C_2Me_2)(S_2C_2Me_2)_2]^{2-}$ (**2**) with 50% probability ellipsoids. Counter ions ($2Et_4N^+$) and hydrogen atoms are omitted for clarity. Selected bond distances (Å) and angles (°) are as follows: W1–O2 1.722(6), W2–O1 1.712(7), W1–S3 2.478(2), W1–S4 2.730(2), W1–S5 2.427(2), W1–S6 2.403(2), W1–S7 2.374(2), W2–S1 2.399(2), W2–S2 2.422(3), W2–S3 2.489(2), W2–S4 2.713(2), W2–S7 2.382(2), W1–W2 2.823(8), W1–S3–W2 69.26(6), W1–S7–W2 72.80(6), and W1–S4–W2 62.48(5).

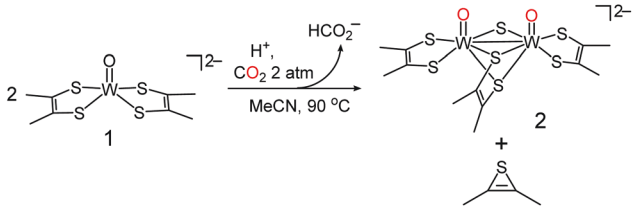

Scheme 1 The structural rearrangement of a mononuclear W complex $[W^{IV}O(S_2C_2Me_2)_2](Et_4N)_2$ (**1**) to a dinuclear complex $[W^{V}_2O_2(\mu\text{-}S)(\mu\text{-}S_2C_2Me_2)(S_2C_2Me_2)_2](Et_4N)_2$ (**2**) under a CO_2 atmosphere along with a concomitant reduction of CO_2 to formate.

The orange-yellow solution of **2** in acetonitrile exhibits distinctive UV-Vis absorption features at 261 (ε = 32 000), 299 (sh, 16 100), 328 (9800), and 396 (7100) nm (Fig. 3a). We assigned the transitions using TD-DFT (time-dependent density functional theory) calculations. A simulated spectrum (Fig. 3b) indicates that the absorption bands are dominated by the ligand-to-metal charge transfers (LMCTs). The strong bands at 261 nm and the 299 nm correlate with the S → W charge transfer. The 328 nm band correlates with the μ-dithiolene → W charge transfer, and the band at 396 nm correlates with the peripheral dithiolene → W charge transfer (Fig. S6†).

The conversion of complex **1** to **2** occurred only when the reaction solution was incubated under a CO_2 atmosphere (Fig. 4a → b). This implies a concomitant reduction of the CO_2 gas. Complex **2** itself does not contain any CO_2-originated carbon. However, we were able to observe a strong peak at 1640 cm^{-1} in the IR spectrum of the crude reaction product, which suggests the presence of a CO_2-derived product (identified as formate, Fig. 4c). To confirm the origin of the 1640 cm^{-1} peak, we used the isotopically labeled $^{13}CO_2$ gas under the same reaction conditions. The IR spectrum of the isotope reaction products showed a new peak at 1595 cm^{-1} along with the abolishment of the 1640 cm^{-1} peak (Fig. 4c). The 45 cm^{-1} wavenumber shift clearly indicates the participation of CO_2 in the reaction. Next, we identified the CO_2-derived product by comparing its ^{13}C NMR spectrum with that of Et_4NHCO_2 in acetonitrile (Fig. S7†). Both spectra of the reaction product and the formate standard gave rise to a ^{13}C NMR peak at 164 ppm, confirming that the product of CO_2 reaction with **1** is the formate (Fig. S8†). In further analysis, the crude reaction solution was treated with ~10 equiv. of HCl (diluted in 1,4-dioxane) in order to protonate the formate. Inspection of the solution with GC-MS (gas chromatography-mass spectrometry) confirmed the presence of formic acid (Fig. S9†).

Another isotope labelling experiment gave us indirect evidence about an intermediate species generated during the reaction. The ^{18}O-labeled CO_2 was used to follow the reaction between W=^{16}O and $C^{18}O_2$. The reaction was stopped after 2 days (as opposed to 4 days) and the reaction mixture was examined by IR spectroscopy. The isotopic shift of formate-carbonyl

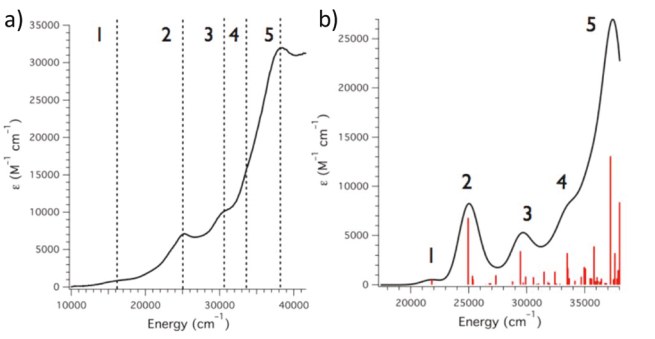

Fig. 3 (a) Experimental, and (b) simulated absorption spectra of complex **2**. The prominent transitions (1–5) are assigned using TD-DFT calculations (Fig. S6†).

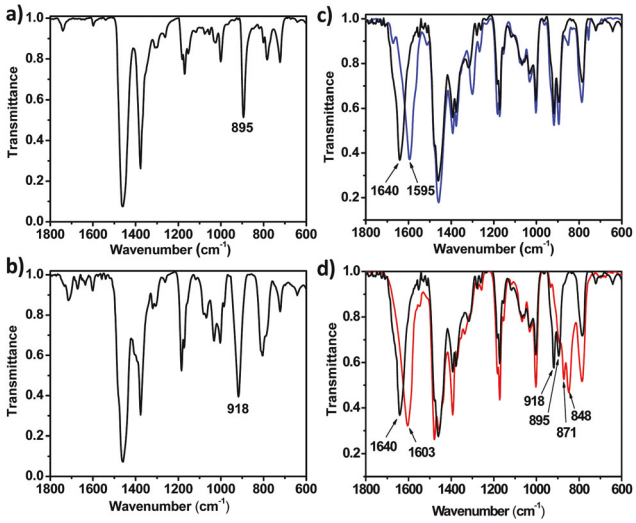

Fig. 4 IR spectra (Nujol) of (a) $[W^{IV}O(S_2C_2Me_2)_2](NEt_4)_2$ (**1**), (b) $[W^{V}_2O_2(\mu\text{-}S)(\mu\text{-}S_2C_2Me_2)(S_2C_2Me_2)_2](NEt_4)_2$ (**2**), (c) the product mixture from the reaction of **1** at 90 °C for 2 days under $^{12}CO_2$ (the black solid line) and $^{13}CO_2$ (the blue solid line), and d) the product mixture from the reaction of **1** at 90 °C for 2 days under $C^{16}O_2$ (the black solid line) and $C^{18}O_2$ (the red solid line).

(1640 → 1603 cm^{-1}) was observed from the reaction between $C^{18}O_2$ and complex **1** as expected. At this time, due to the incomplete reaction resulting from a shorter reaction time, an interesting insight was gained. We observed that both the W=O peaks of complexes **1** and **2** were shifted, as complex **1**: 895 → 848 cm^{-1} and complex **2**: 918 → 871 cm^{-1} (Fig. 4d). This indicates that W=^{16}O of **1** exchanges its oxygen atom with those from $C^{18}O_2$ possibly through a W-carbonate intermediate. This reactivity pattern is similar to that of our previously reported system[26] and is reminiscent of the computational study of the enzyme W-FDH active site which suggests the formation of a W-thiocarbonate intermediate.[27]

For the generation of formate from the reaction of **1**/CO_2, a proton source is necessary. Although we cannot completely rule out the acetonitrile solvent as a proton source, we suspected that a trace amount of water in the solvent would be a source for the proton because there is no strong base in the reaction mixture. Therefore, we re-examined the reaction by adding water (5%) into the reaction in acetonitrile. The reaction, however, did not result in the formate nor in complex **2**. Rather, it yielded a green decomposed species, fully oxidized inorganic W-oxides, consistent with the known proton/moisture sensitivity of the W^{IV}=O species.[34] This result suggests that the proton delivery into the catalytic site must take place in a controlled manner for an efficient conversion of CO_2 to formate. Indeed, the W-FDHs have highly conserved amino acid residues (SeCys^{140}–CH_2–Se–H) in the secondary coordination sphere of the CO_2 binding site which can regulate the supply of protons to the (thio)carbonate intermediate in a sophisticated manner.[27] Another important difference between the enzyme active site and the current synthetic model is an incomplete structural mimic of the pyranopterin-

dithiolate ligand, MPT (Fig. 1). The ligand used in our model compound pertains only to the dithiolene moiety, the primary coordination environment. However, the MPT ligand found in the enzyme is a dithiolene that is fused with the redox-active pterin moiety, which can play an important role in enzyme catalysis.[35,36] It is conceivable that the presence of the pterin moiety in the ligand periphery might prevent the unwanted bond cleavage of the ligand observed in our model compound. Indeed, a recently reported Ni bis(dithiolene) electrocatalyst capable of converting CO_2 to formate employs an MPT analogue, in which opening of the pyran ring of the ligand is a critical feature to achieve catalytic activity.[37]

In summary, we have demonstrated a novel CO_2 reactivity of the bis-dithiolene W^{IV}=O complex, a biomimetic complex for the active site of the W-dependent formate dehydrogenase (W-FDH). The reported bis-dithiolene W^{IV}=O complex reduces gaseous CO_2 to formate at 90 °C, while W^{IV}=O becomes oxidized by CO_2 to form an unprecedented triply bridged dinuclear W^{V}=O dithiolene complex. These results provide insights into the importance of the secondary coordination environment and the synthetic strategies for biomimetic CO_2 reduction catalysts. The features of the biomimetic FDH catalysts in the next generation would include a proton delivery moiety and a dithiolene appended by pterin moieties in the ligand.

Conflicts of interest

There are no conflicts of interest to declare.

Acknowledgements

This work was supported by a GIST Research Institute (GRI) grant funded by the GIST in 2019, the Basic Science Research Program through the National Research Foundation of Korea (NRF) funded by the Ministry of Education (2018R1C1B5047260), and the US National Science Foundation (1807845).

References

1 Q.-W. Song, Z.-H. Zhou and L.-N. He, *Green Chem.*, 2017, **19**, 3707.
2 M. Beller and U. T. Bornscheuer, *Angew. Chem., Int. Ed.*, 2014, **53**, 4527.
3 T. Sakakura, J.-C. Choi and H. Yasuda, *Chem. Rev.*, 2007, **107**, 2365.
4 E. E. Benson, C. P. Kubiak, A. J. Sathrum and J. M. Smieja, *Chem. Soc. Rev.*, 2009, **38**, 89.
5 J. Qiao, J. Qiao, Y. Liu, F. Hong and J. Zhang, *Chem. Soc. Rev.*, 2014, **43**, 631.
6 M. Álvarez, A. Galindo, P. J. Pérez and E. Carmona, *Chem. Sci.*, 2019, **10**, 8541.
7 S. A. Gonsales, I. Ghiviriga, K. A. Abboud and A. S. Veige, *Dalton Trans.*, 2016, **45**, 15783.
8 S. Chakraborty, O. Blacque and H. Berke, *Dalton Trans.*, 2015, **44**, 6560.
9 R. G. Carden, J. J. Ohane, R. D. Pike and P. M. Graham, *Organometallics*, 2013, **32**, 2505.
10 J. M. Wolfe and W. H. Bernskoetter, *Dalton Trans.*, 2012, **41**, 10763.
11 G. R. Lee, J. M. Maher and N. J. Cooper, *J. Am. Chem. Soc.*, 1987, **109**, 2956.
12 B. D. Ward, G. Orde, E. Clot, A. R. Cowley, L. H. Gade and P. Mountford, *Organometallics*, 2005, **24**, 2368.
13 J. M. Maher and N. J. Cooper, *J. Am. Chem. Soc.*, 1980, **102**, 7604.
14 D. J. Darensbourg, K. M. Sanchez, J. H. Reibenspies and A. L. Rheingold, *J. Am. Chem. Soc.*, 1989, **111**, 7094.
15 T. Ishida, T. Hayashi, Y. Mizobe and M. Hidai, *Inorg. Chem.*, 1992, **31**, 4481.
16 D. J. Darensbourg and C. Ovalles, *J. Am. Chem. Soc.*, 1984, **106**, 3750.
17 H. Raaijmakers, S. Macieira, J. M. Dias, S. Teixeira, S. Bursakov, R. Huber, J. J. G. Moura, I. Moura and M. J. Romão, *Structure*, 2002, **10**, 1261.
18 T. Reda, C. M. Plugge, N. J. Abram and J. Hirst, *Proc. Natl. Acad. Sci. U. S. A.*, 2008, **105**, 10654.
19 A. Bassegoda, C. Madden, D. W. Wakerley, E. Reisner and J. Hirst, *J. Am. Chem. Soc.*, 2014, **136**, 15473.
20 S. Groysman and R. H. Holm, *Inorg. Chem.*, 2007, **46**, 4090.
21 J. Jiang and R. H. Holm, *Inorg. Chem.*, 2004, **43**, 1302.
22 C. A. Goddard and R. H. Holm, *Inorg. Chem.*, 1999, **38**, 5389.
23 K.-M. Sung and R. H. Holm, *Inorg. Chem.*, 2001, **40**, 4518.
24 S. Khatua, T. Naskar, C. Nandi and A. Majumdar, *New J. Chem.*, 2017, **41**, 9769.
25 S. Sarkar and S. K. Das, *Proc. – Indian Acad. Sci., Chem. Sci.*, 1992, **104**, 533.
26 J. Seo and E. Kim, *Inorg. Chem.*, 2012, **51**, 7951.
27 C. S. Mota, M. G. Rivas, C. D. Brondino, I. Moura, J. J. G. Moura, P. J. González and N. M. F. S. A. Cerqueira, *J. Biol. Inorg. Chem.*, 2011, **16**, 1255.
28 G. Dong and U. Ryde, *J. Biol. Inorg. Chem.*, 2018, **23**, 1243.
29 A. Döring and C. Schulzke, *Dalton Trans.*, 2010, **39**, 5623.
30 M. K. Johnson, *Prog. Inorg. Chem.*, 2004, **52**, 213.
31 B. S. Lim, D. V. Fomitchev and R. H. Holm, *Inorg. Chem.*, 2001, **40**, 4257.
32 F. Bigoli, C.-T. Chen, W.-C. Wu, P. Deplano, M. L. Mercuri, M. A. Pellinghelli, L. Pilia, G. Pintus, A. Serpe and E. F. Trogu, *Chem. Commun.*, 2001, 2246.
33 S. Sproules and K. Wieghardt, *Coord. Chem. Rev.*, 2010, **254**, 1358.
34 J. Seo, P. G. Williard and E. Kim, *Inorg. Chem.*, 2013, **52**, 8706.
35 D. R. Gisewhite, J. Yang, B. R. Williams, A. Esmail, B. Stein, M. L. Kirk and S. J. N. Burgmayer, *J. Am. Chem. Soc.*, 2018, **140**, 12808.
36 P. Basu and S. J. N. Burgmayer, *Coord. Chem. Rev.*, 2011, **255**, 1016.
37 T. Fogeron, T. K. Todorova, J.-P. Porcher, M. Gomez-Mingot, L.-M. Chamoreau, C. Mellot-Draznieks, Y. Li and M. Fontecave, *ACS Catal.*, 2018, **8**, 2030.